2005 American Control Conference
June 8-10, 2005. Portland, OR, USA

Optimal Velocity Profile Generation for Given Acceleration Limits: Receding Horizon Implementation

Efstathios Velenis* and Panagiotis Tsiotras*

Abstract— **We present a semi-analytical method to generate the optimal velocity profile for a vehicle traveling along a prescribed path in minimum time, given a maximum acceleration limit. A receding horizon implementation is proposed for the on-line implementation of the velocity optimizer. Robustness of the receding horizon algorithm is guaranteed by the use of a dynamic scheme that determines the planning and execution horizons. Application to a real-life scenario provides a validation of the proposed methodology. A comparison between the infinite and finite receding horizon schemes is also presented.**

I. Introduction

The problem of trajectory planning for high-speed autonomous vehicles is typically dealt with in the literature by means of numerical optimization. Several results have been published recently that address path planning of high-speed ground vehicles [1], [2], [3], [4]. These results demonstrate that numerical techniques allow one to incorporate accurate, high order dynamical models in the optimization process, thus producing realistic results. In fact, the optimal solutions generated using these optimizers are comparable to experimental results obtained from expert race drivers. On the other hand, these numerical optimization approaches are computationally costly, and they cannot be readily applied to unpredictably changing environments. As a result, they may not be applicable to real-time path-planning optimization scenarios.

In [5], [6], [7] real-time trajectory planning of autonomous (aerial) vehicles using a receding horizon scheme was proposed. In receding horizon, the optimization is not performed throughout the whole trajectory, but rather from the current position up to a pre-specified horizon. The vehicle executes part of the computed optimal trajectory while simultaneously optimizing the path up to a new horizon. This allows trajectory planning to be applied on-line, since the optimization search space is considerably reduced, thus reducing the computational cost as well. The method also allows changing environments or moving obstacles to be incorporated.

An alternative approach for on-line trajectory optimization of ground vehicles is proposed in this work. Having in mind the reduction of the computational cost, we are motivated to explore the possibility of solving the trajectory planning problem (or at least part of the problem) analytically. We separate the geometric problem of designing the optimal path from the dynamic problem of optimally following this path given the vehicle dynamic characteristics. Specifically, we assume that the geometric characteristics of the reference trajectory are provided to us. This means that the path to be followed will be the result of another optimization step, which will typically incorporate additional constraints such as minimum distance traveled, minimum average curvature, or a combination of the two. Since the dynamics of the vehicle are not directly included in this optimization step we expect a reduced computational cost.

The path-following part of the optimization consists of the calculation of the optimal velocity profile through the prescribed path given the dynamics of the vehicle. A semi-analytical method that provides an intuitively optimal velocity profile was proposed in [8] and [9]. A formal proof of optimality of this methodology has been provided in [10]. In the same reference several uncontrollable cases, which were neglected in [8] and [9], were completely analyzed. Suboptimal alternatives to treat these uncontrollable cases were also proposed.

In this paper, we first review the methodology of [8], [9] and [10] to generate the optimal velocity profile on a prescribed path for the minimum time travel of a vehicle with given acceleration limits. The application of this methodology and comparison with lap times of race drivers on an actual trajectory of a race car through an F1 circuit provides validation of the method. Finally, we introduce a receding horizon implementation in order to incorporate unpredictable changes in the environment. The planning and execution horizons are selected via a dynamic scheme that depends of the current vehicle velocity. The scheme ensures the robustness of the receding horizon implementation.

II. Optimal Velocity Profile

Consider a vehicle of mass m traveling through a prescribed path, given acceleration limits and fixed boundary conditions. We investigate the velocity profile of the vehicle through the path for minimum time travel. The path is described by the radius at each point as a function of the path length coordinate s, $R(s)$ (Fig. 1), or equivalently, by the curvature $k(s)$. The cartesian coordinates of any point on the path may be calculated using the following transformation [3]

$$k(s) = \frac{1}{R(s)}, \tag{1}$$

$$\psi(s) = \int_0^s k(s)\mathrm{d}s, \tag{2}$$

* School of Aerospace Engineering, Georgia Institute of Technology, Atlanta, GA 30332-0150, USA, {efstathios_velenis,p.tsiotras}@ae.gatech.edu

0-7803-9098-9/05/$25.00 ©2005 AACC

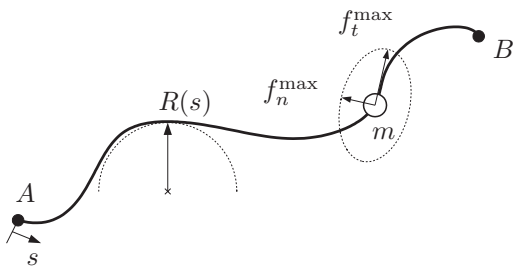

Fig. 1. A vehicle of mass m travels along the prescribed path $R(s)$, given maximum acceleration limits, in minimum time.

$$x(s) = \int_0^s \cos(\psi(s))\mathrm{d}s, \tag{3}$$

$$y(s) = \int_0^s \sin(\psi(s))\mathrm{d}s. \tag{4}$$

The equations of motion are given by

$$m\frac{\mathrm{d}^2 s}{\mathrm{d}t^2} = f_t \ , \quad \frac{m\left(\frac{\mathrm{d}s}{\mathrm{d}t}\right)^2}{R(s)} = f_n \tag{5}$$

where, f_t is the force tangential to the path, and f_n is the force normal to the path. We assume that the path is followed exactly by the vehicle, therefore the normal force f_n is given by (5). The control input is the longitudinal force f_t. The given acceleration limits result in the following control constraint

$$\left(\frac{f_t}{f_t^{\max}}\right)^2 + \left(\frac{f_n}{f_n^{\max}}\right)^2 - 1 \leq 0, \tag{6}$$

where $f_t^{\max}$ is the maximum longitudinal force and $f_n^{\max}$ the maximum lateral force, respectively. Introducing a new control variable u, the control constraint (6) may be rewritten as follows

$$f_t = u\sqrt{(f_t^{\max})^2 - \frac{m}{R}\left(\frac{f_t^{\max}}{f_n^{\max}}\right)^2\left(\frac{\mathrm{d}s}{\mathrm{d}t}\right)^2} \tag{7}$$

where $u \in [-1, +1]$.

Assuming that the trajectory remains inside a region where controllability is maintained and the dynamics are well defined, it is proven in [10] that for minimum time travel, the maximum available force is used at all times, that is, the optimal control consists only of subarcs of full acceleration ($u = +1$) or full deceleration ($u = -1$).

Note that there exists a critical velocity

$$\frac{\mathrm{d}s}{\mathrm{d}t} = v_{\text{critical}} = f_n^{\max}\sqrt{\frac{R}{m}} \tag{8}$$

for which $f_t = 0$. In this case $f_n = f_n^{\max}$ and the total acceleration of the vehicle is used to produce the required centripetal force. As a result, no available force remains for longitudinal acceleration/deceleration, and loss of controllability ensues. Clearly, the velocity v_{critical} is the maximum allowable velocity at each point of the path. The reader is referred to [10] for a detailed discussion.

The optimal velocity profile in [10] is constructed as follows.

Step 1: Certain points of interest along the path are identified. These are the points where the radius has a local minimum and the parts of the path with constant radius. Let us consider a path with a radius profile as in Fig. 2. The points of interest are the local minima of the radius profile, that is, points P_1, P_2 and P_5, and the part of the radius profile between points P_3 and P_4 of constant radius.

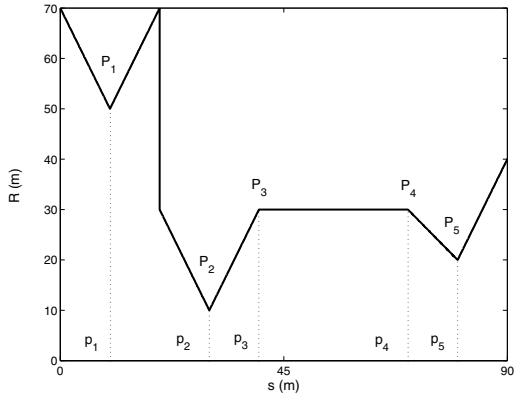

Fig. 2. A general radius profile.

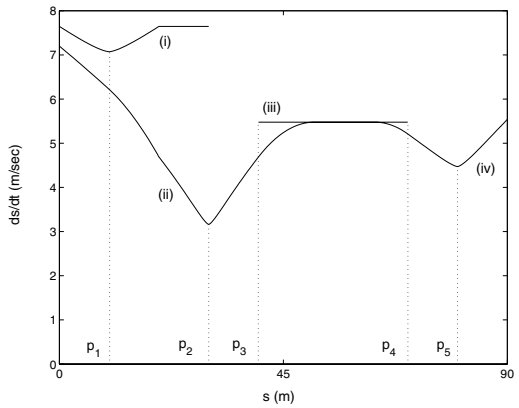

Fig. 3. The solutions for the free-boundary problem for the subarcs of constant radius and $\min R$.

Step 2: We calculate the optimal velocity profile for each of the subarcs containing the points of interest subject to free boundary conditions. For the subarcs containing a unique point of local minimum radius, this profile consists of full deceleration ($u = -1$) before, and full acceleration ($u = +1$) after the local minimum. The velocity at each local minimum is equal to the corresponding v_{critical}. In Fig. 3 the characteristic (i) corresponds to point P_1, the characteristic (ii) corresponds to point P_2, and the characteristic (iv) to point P_5. For the subarcs of constant radius, the free-boundary condition profile consists of constant velocity as close to (but not equal to) v_{critical} as possible. In

Fig. 3 the characteristic profile (iii) corresponds to the part between points P_3 and P_4.

Step 3: For the given boundary conditions, (points A and B in Fig. 4) we construct the characteristic velocity profile of full acceleration ($u = +1$) from the initial point (i.e., the characteristic (I) in Fig. 4)), and the characteristic profile of full deceleration ($u = -1$) towards the final point (i.e., the characteristic (II) in Fig. 4).

Step 4: The optimal velocity at each point of the path is the minimum of all the above characteristic velocity profiles at that point. For the example under consideration, this is $v^*(s) = \min\{v^k(s)\},\ k = \mathrm{i}, \mathrm{ii}, \mathrm{iii}, \mathrm{iv}, \mathrm{I}, \mathrm{II}$, with $v^k(s)$ the velocity profile corresponding to the kth characteristic. This optimal velocity profile is depicted by a solid line in Fig. 4.

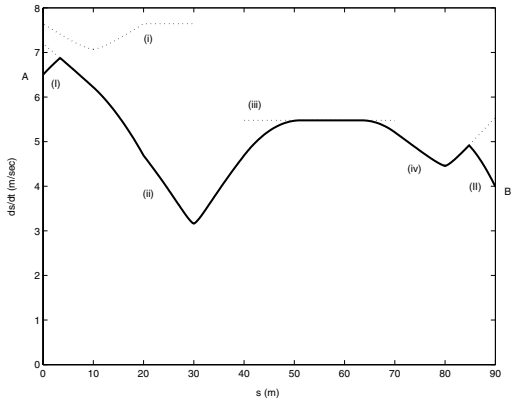

Fig. 4. Optimal velocity for the radius profile of Fig. 2.

III. Application on an F1 circuit

In this section we validate the proposed methodology by applying it to an actual road track. Specifically, we use the previous methodology to generate the optimal velocity profile over an F1 circuit, given the acceleration limits of a typical F1 race car. The results are compared to the velocity profiles and lap times achieved by expert F1 race drivers.

Figure 5, taken from [11], shows the cartesian coordinates of the Silverstone F1 circuit. The data of Fig. 5 along with the inverse of the transformation (1)-(4) were used to generate the radius profile of this trajectory, which is shown in Fig. 6.

By roughly matching the performance characteristics of the vehicles in [3], [11] we may approximate the acceleration limits of a typical F1 race car as follows

$$f_t^{\max}/m = \begin{cases} +16 - 0.0021v^2 \ \mathrm{m/sec^2} \text{ for } u = +1 \\ -18 - 0.0021v^2 \ \mathrm{m/sec^2} \text{ for } u = -1 \end{cases}$$
$$f_n^{\max}/m = 30 \mathrm{m/sec^2}$$

The optimal velocity profile along the trajectory of Fig. 5 was then calculated using the methodology of Section II. The results are shown in Fig. 7 (bottom). Figure 7 (top),

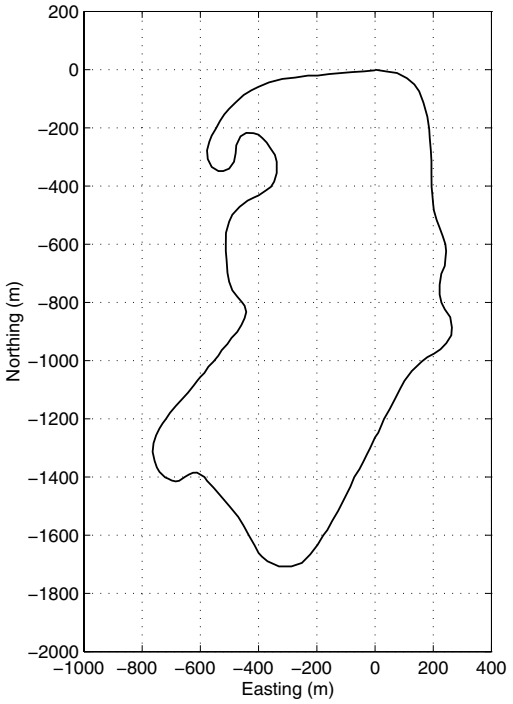

Fig. 5. The Silverstone F1 circuit [11].

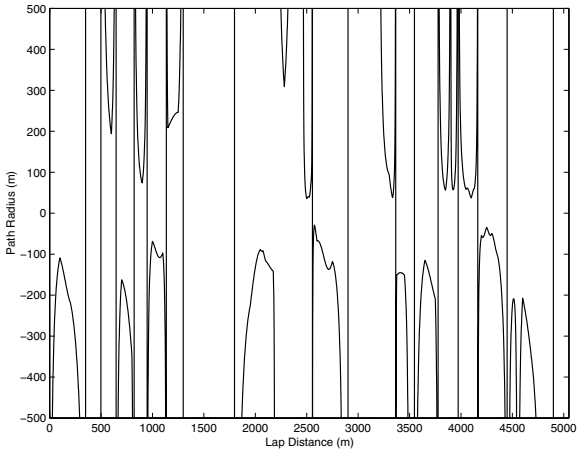

Fig. 6. Radius profile along the trajectory of Fig. 5.

taken from [11], shows the velocity measurements for three laps of an F1 car along the Silverstone circuit. The optimally calculated lap time is $82.7\,\mathrm{sec}$ and the measured lap times corresponding to the data of Fig. 7 (top) are $86.063\,\mathrm{sec}$, $90.891\,\mathrm{sec}$ and $85.805\,\mathrm{sec}$ respectively for each lap. Note that the record time for the Silverstone circuit belongs to J. Montoya ($78.998\,\mathrm{sec}$, Williams, 2002).

IV. Optimization using Receding Horizon

As already mentioned, a key element for a trajectory planning scheme for autonomous vehicles is the ability to incorporate unpredictably changing environments. To this end, trajectory optimization is often implemented in a receding horizon scheme rather than executed in one

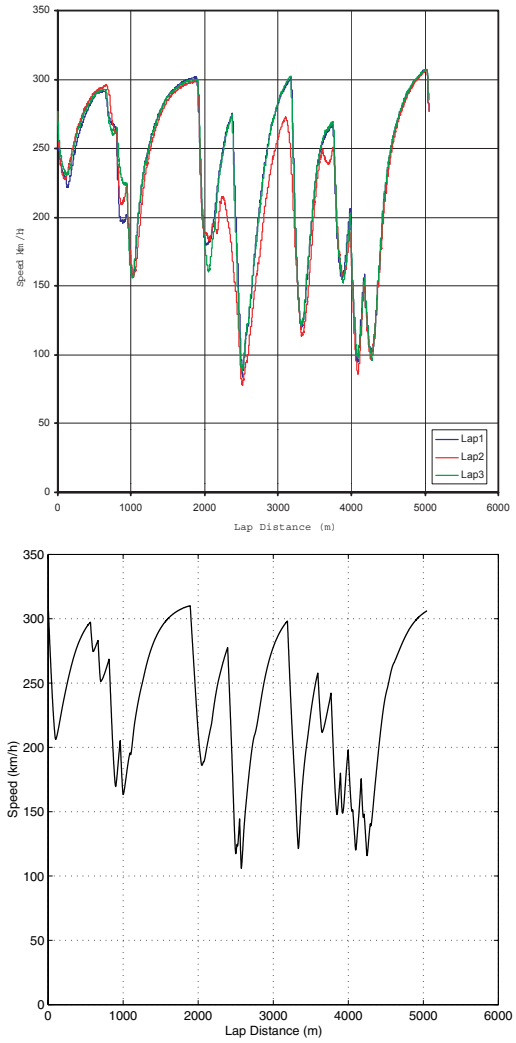

Fig. 7. Velocity profiles for the Silverstone circuit: experimental (top), computed optimal (bottom).

shot, from the starting to the end point. In [5] numerical optimization along with a receding horizon scheme was used for trajectory planning of an autonomous vehicle maneuvering through obstacles. By including the distance between the horizon and the final destination point in the total cost it was shown that the vehicle reaches the final point. In [6] an extension of the previous optimization scheme was proposed in order to avoid the entrapment of the vehicle in concave obstacles. The main idea is that the cost function is estimated off-line for the whole area where the vehicle may move. Areas that may lead to entrapment are penalized and the estimated cost is taken into consideration in the total cost. Finally, in [7] the receding horizon strategy of [5] was combined with a "safety algorithm". The "safety algorithm" computes an "escape" plan from the end of the horizon to a "safe" state (such as the vehicle coming to a stop), for each optimization step. If such an "escape plan" is not feasible, then the last optimization step is not executed and the "escape plan" of the previous step is executed instead.

In this work we have assumed that the geometry of the trajectory is computed separately and it is provided to the velocity optimizer beforehand. Therefore, during a receding horizon implementation we assume that it is the job of the path planner to provide a feasible path that ensures obstacle avoidance and guarantees that the vehicle will reach its final destination. This can be achieved by following the same strategy as in [5],[6] and [7]. However, guarantees that the velocity will not exceed the critical value at any point and that there exists an "escape" plan at the end of each optimization step will have to be provided before the optimal velocity profile generator is implemented in a receding horizon scheme. In this paper we propose a dynamic scheme to adaptively choose the planning and execution horizons to provide such guaranties.

In the following, we summarize the key ideas of the receding horizon implementation of the optimal velocity generator.

A. Basic Notions

Figure 8 shows a schematic that demonstrates how the receding horizon scheme works. The *Planning Horizon* (PH) is the distance from the current position up to the point which the optimization is performed. The *Execution Horizon* (EH) is a fraction of (PH) and it is the distance up to the point which the planned optimization will actually be executed. When the vehicle reaches the *Replanning Horizon* (RH), which is a fraction of (EH), the optimization is performed again up to the new planning horizon.

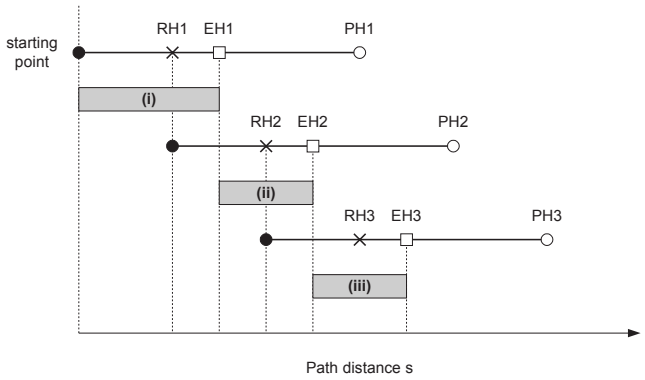

Fig. 8. Optimization with receding horizon.

Let the vehicle be at the starting point ($s = 0$ in Fig. 8). The optimization methodology is applied up to (PH1). After the optimization is completed, the vehicle may start executing the optimal trajectory up to (EH1). The shadowed area (i) in Fig. 8 shows the portion of the first optimization that is actually executed. When the vehicle reaches (RH1) the optimization is applied again from the current position (RH1) to the new planning horizon (PH2). The portion of the second optimization that will actually be executed is from (EH1) to (EH2) and it is shown as the shadowed area (ii) in Fig. 8. The process will end when the final

destination is within the execution horizon. The distance between (RH) and (EH) is chosen such that enough time is allowed for the computation of the optimal trajectory from (RH) to the next (PH) before (EH) is reached. If the computation was instantaneous (RH) and (EH) could be the same. As already mentioned, the semi-analytical nature of the proposed algorithm results in little computational cost and thus from now on we will assume that the replanning and execution horizons coincide.

B. Robustness guarantees

The choice of (PH) and (EH) is crucial for the success of the receding horizon optimization scheme. The difference between (EH) and (PH) has to be large enough so that there is enough time to correct the executable trajectory each time a new optimization is completed.

Consider the path of Fig. 2 and the several solutions resulting from a receding horizon optimization scheme of the velocity shown in Fig. 9. Let the planning horizon be chosen as (PH0), which coincides with the end of the increasing curvature subarc after the point P_1 (cf. Fig. 2). This implies that the decreasing curvature subarc before point P_2 is outside the planning horizon. Assume that the execution horizon be (EH0) as shown in Fig. 9. The optimal solution for this case is to accelerate until the characteristic profile (i), and then follow the characteristic (i). The execution horizon being at (EH0) results in the vehicle reaching point P_1 with velocity greater than the optimal one, as shown in Fig. 4. This means that the vehicle will not be able to decelerate strongly enough to negotiate the minimum radius point at P_2 and hence the vehicle will leave the prescribed path.

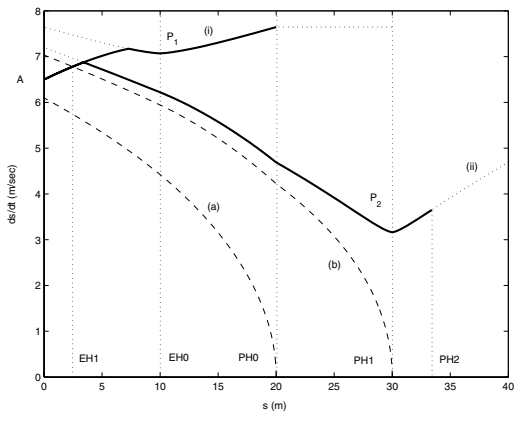

Fig. 9. Dynamic scheme for (EH) determination.

Next, we propose a dynamic scheme to choose (EH) which guarantees fail-safe operation of the receding horizon implementation. Assume that for the previous example we choose the planing horizon to be at (PH1) as in Fig. 9. The optimal solution up to (PH1) is acceleration until the characteristic (ii) is reached, followed by staying on (ii) using full deceleration. Using backward integration we find the characteristic (b) (refer to in the sequel as the "emergency stop" characteristic) of full deceleration to zero velocity at (PH1). As execution horizon we choose the point where the characteristic (b) intersects the optimal solution calculated, that is (EH1). This means that of the whole optimal solution calculated, only the part up to (EH1) is executed. Although (EH1) is much shorter that (PH1), we nonetheless guarantee that after the execution of the optimal trajectory up to (EH1) we are left with enough distance so that the vehicle comes to a complete stop at (PH1). This stopping condition is achieved regardless of the path that follows (PH1).

Note that for the proposed scheme to work, the planning horizon has to be long enough for the "emergency stop" characteristic to intersect the optimal solution within the planning horizon. In fact, for the first example where the choice of (PH) and (EH) led to failure of the receding horizon implementation, this criterion was not satisfied. For this case the "emergency stop" characteristic, (a) in Fig. 9, does not intersect the optimal solution within the planning horizon. A longer planning horizon is required for fail-safe operation.

Furthermore, note that, in contrast to the "safety algorithm" proposed in [7] (where each "escape plan" is calculated from the end point of the planning horizon) our approach does not require any information outside the planning horizon.

The choice of (PH) is still left free as long as it satisfies the requirement that the "emergency stop" characteristic intersects the optimal solution within the planning horizon. We can therefore choose (PH) using a dynamic scheme that depends on the velocity of the vehicle at the end of (EH). Specifically, we choose

$$(\mathrm{PH}) = \max\{Tv, (\mathrm{PH})_{\min}\} \tag{9}$$

where v is the vehicle velocity, T is a constant "reaction" time, and $(\mathrm{PH})_{\min}$ is the minimum planning horizon (typically for $v = 0$). This is not unlike the way a human driver chooses a planning horizon, that is, the larger the velocity, the longer the "look ahead" distance needs to be. In case the "emergency stop" characteristic does not intersect the optimal solution within the planning horizon, a larger T must be chosen.

C. Numerical Example

In this section we apply the proposed receding horizon algorithm to the F1 car trajectory of Section III. We have chosen $T = 5$ sec, which for this example is enough for the "emergency stop" characteristic to intersect the optimal solution within the planning horizon for each iteration. The minimum planning horizon was chosen as $(\mathrm{PH})_{\min} = 200$ m.

In Fig. 10 the results of the first five steps of the receding horizon scheme are shown, along with the planning and execution horizons of each step. The solution (solid line) is compared with the infinite-horizon solution of the optimal velocity generator of Section III (dotted line). The

two solutions coincide, thus confirming the validity of the proposed receding horizon scheme.

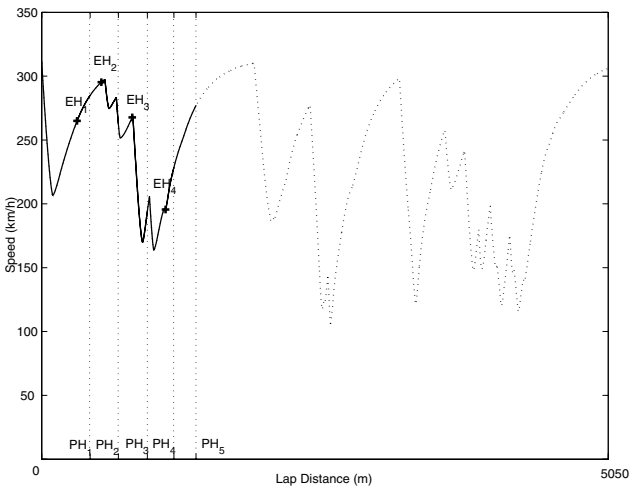

Fig. 10. Optimization with receding horizon of the Silverstone circuit.

V. CONCLUSIONS

A receding horizon implementation of a semi-analytical method to generate the minimum-time, optimal velocity profile of a vehicle traveling on an arbitrarily prescribed path for given acceleration limits is proposed. The low computational cost of the proposed analytic approach, along with the inherent capability of receding horizon schemes to incorporate unpredictable changes in the environment makes the approach suitable for on-line implementation. To ensure robustness and the existence of an "escape plan" without any information outside the planning horizon, a dynamic scheme is proposed to determine the execution and planning horizons at each step. Validation of both infinite and receding horizon implementations is provided by applying them to the Silverstone F1 circuit. The results showed that the proposed on-line velocity optimizer is very competitive when compared to lap times obtained by expert F1 race drivers.

Acknowledgment: This work has been supported in part by the US Army Research Office, award no. DAAD19-00-1-0473.

REFERENCES

[1] T. Fujioka and M. Kato, "Numerical analysis of minimum-time cornering," in *Proceedings of AVEC 1994*, November 24-28 1994, Tsukuba, Japan.

[2] J. Hendrikx, T. Meijlink, and R. Kriens, "Application of optimal control theory to inverse simulation of car handling," *Vehicle System Dynamics*, vol. 26, pp. 449–461, 1996.

[3] D. Casanova, R. S. Sharp, and P. Symonds, "Minimum time manoeuvring: The significance of yaw inertia," *Vehicle System Dynamics*, vol. 34, pp. 77–115, 2000.

[4] ——, "On minimum time optimisation of formula one cars: The influence of vehicle mass," in *Proceedings of AVEC 2000*, August 22-24 2000, ann-Arbor, MI.

[5] T. Schouwenaars, B. De Moor, E. Feron, and J. How, "Mixed integer programming for multi-vehicle path planning," in *Proceedings of the 2001 European Control Conference*, September 2001, Porto, Portugal.

[6] J. Bellingham, A. Richards, and J. How, "Receding horizon control of autonomous aerial vehicles," in *Proceedings of the American Control Conference*, May 8-10 2002, Anchorage, AK.

[7] T. Schouwenaars, E. Feron, and J. How, "Safe receding horizon path planning for autonomous vehicles," in *Proceedings of the 40th Allerton Conferenceon Communication, Control and Computing*, October 2002, Monticello, IL.

[8] M. Gadola, D. Vetturi, D. Cambiaghi, and L. Manzo, "A tool for lap time simulation," in *Proceedings of SAE Motorsport Engineering Conference and Exposition*, 1996, Dearborn, MI.

[9] M. Lepetic, G. Klancar, I. Skrjanc, D. Matko, and B. Potocnic, "Time optimal path planning considering acceleration limits," *Robotics and Autonomous Systems*, vol. 45, pp. 199–210, 2003.

[10] E. Velenis and P. Tsiotras, "Optimal velocity profile generation for given acceleration limits: Theoretical analysis," in *Proceedings of the American Control Conference*, June 8 - 10 2005, Portland, OR.

[11] Anonymous, "RT3000 inertial and GPS measurement system, report from Silverstone F1 test," Oxford Technical Solutions, Oxfordshire, UK, Technical Report, 2002.